

Fabrication of spindle Fe_2O_3 @polypyrrole core/shell particles by surface-modified hematite templating and conversion to spindle polypyrrole capsules and carbon capsules

Shouhu Xuan^{a,b}, Qunling Fang^b, Lingyun Hao^{b,c}, Wanquan Jiang^b, Xinglong Gong^c, Yuan Hu^{a,*}, Zuyao Chen^b

^a State Key Laboratory of Fire Science, The University of Science and Technology of China (USTC), Hefei, Anhui 230026, PR China

^b Department of Chemistry, USTC, Hefei 230026, PR China

^c Key Laboratory of Mechanical Behavior and Design of Materials, Department of Mechanics and Mechanical Engineering, USTC, Hefei 230026, PR China

Received 31 January 2007; accepted 17 May 2007

Available online 23 May 2007

Abstract

By using a surface-modified templating method, Fe_2O_3 @polypyrrole (PPy) core/shell spindles have been successfully prepared in this paper. The Fe_2O_3 particles with spindle morphology were initially fabricated as core materials. After the PVP modification, the Fe_2O_3 spindles were subsequently coated with a tunable thickness layer of PPy by in situ deposition of the conducting polymer from aqueous solution. Hollow PPy spindles were produced by dissolution of the Fe_2O_3 core from the core/shell particles. High-temperature treatment under vacuum condition convert the hollow PPy spindles into carbon capsules by carbonization of the PPy shell. Transmission electron microscope (TEM), scanning electron microscopy (SEM), Fourier transform infrared spectroscopy (FTIR), thermal gravimetric analysis (TGA) and X-ray photoelectron spectroscopy (XPS) confirmed the formation of the Fe_2O_3 @PPy core/shell particles, PPy and carbon capsules with spindle morphology.

© 2007 Elsevier Inc. All rights reserved.

Keywords: Core/shell; Fe_2O_3 ; Polypyrrole; Spindle; Carbon

1. Introduction

Considerable efforts have been devoted to the design and controlled fabrication of core/shell structure particles, since these particles show some special properties in optics, electronics, magnetics and catalysis by adjusting their size, chemical composition and structure order [1,2]. The Hollow capsules are another important class of materials commonly coming from the core/shell particles by direct removal of the cores [3,4]. These hollow spheres can be utilized widely in areas of medicine, pharmaceuticals, agricultures, and cosmetics [5,6]. The vast majority of the applications are associated with the controlled release of encapsulated active ingredients (e.g. drugs, vaccines, antibodies, hormones, pesticides, and fragrances) under

well defined conditions. Many techniques such as the layer-by-layer deposition technique [7], in situ polymerization on template particles [8] pH-induced micellization of grafted copolymer [9], and core-free-template strategy [10] have been developed to prepare core/shell structure particles and hollow capsules whose size ranges from tens of nanometers to a few micrometers.

Recently, conductive polymer core/shell composites and hollow capsules have been intensively focused on owing to their wide variety of applications [11]. The list involves encapsulation of products (for the controlled release of drugs, cosmetics, inks, and dyes), the protection of light sensitive components, catalysis, coatings, composites, and transplantation of cell and enzyme, removal of contaminated waste, gene therapy, and heterogeneous catalysis [12]. Armes and co-workers have carried out pioneer studies on stable colloidal conducting polymer core/shell nanocomposites using a technique for encapsulating colloidal particles with PPy or polyaniline [13,14].

* Corresponding author. Fax: +86 551 3601664.
E-mail address: yuanhu@ustc.edu.cn (Y. Hu).

And very recently, inspired by the space science observations, they designed new conducting polymer-coated sulfur-rich latex particles to be employed as new synthetic mimics so as to understand the fundamental impact ionization behavior of sulfur-based micrometeorites in laboratory-based studies [15]. Among these conducting polymers, PPy is one of the most extensively studied materials due to its good environmental stability, high conductivity and biocompatibility [16]. For example, strong DNA adsorption onto polypyrrole (PPy) powders has been investigated at an appropriate condition [17]. The study of adsorption of polymers onto PPy showed that this conducting polymer has high surface energy and strong acid–base interactions with macromolecule [18]. To date, various inorganic or organic core and PPy shell nanostructures such as SiO_2 @PPy, PS@PPy and AgBr@PPy–chitosan with sphere-like [13,19], sunflower-like [20], cube-like and plate-like [21] have been successfully synthesized. Despite a massive amount of work on the synthesis and characterization of colloidal particles coated with PPy shells and their corresponding hollow capsules, only a few works have reported about non-spherical core/shell particles and hollow capsules, because of the lack of non-spherical templates [22]. Non-spherical colloids and their ordered arrays may be more attractive in applications than their spherical counterparts because of their lower symmetries. Therefore, it is still worth finding other core/shell nanoparticles with lower symmetries for most of which have been reported are spherical. Further more, owing to the high specific surface area, large pore volume, chemical inertness and good mechanical stability [23], carbon nanocapsules which can be fabricated by the carbonization of the polymeric capsules, have attracted more and more intense interest [24,25]. Hence, the development of synthesis strategy for the non-spherical polymer capsules and the conversion to carbon hollow nanostructure has become a pressing need not only for the fundamental interest but also for their high efficiency and facility.

It is difficult to directly coat sub-micron sized hematite with a polymer due to heavy flocculation. With silica shells, hematite particles were better coated with many functional materials. Previously, our group had reported the fabrication and characterization of sandwich Fe_2O_3 @ SiO_2 @PPy ellipsoidal particles and four kind of hollow capsules [26]. However, it is still a challenge to find tactics for directly preparing anisotropic Fe_2O_3 @PPy core/shell particles. Since Fe_2O_3 is initially hydrophilic, it is very difficult to form the hydrophobic PPy shell on Fe_2O_3 by direct surface polymerization. Moreover, because of the variation in curvature across the surface of a non-spherical particle; it would be more difficult to directly coat a non-spherical template than a spherical one.

In the present work, we aim to report new results along these lines on the synthesis of a novel non-spherical conducting inorganic/polymer composite. To the best knowledge of our, this is the first report about the fabrication of spindle Fe_2O_3 @PPy core/shell composites by directly in situ chemical polymerization of pyrrole monomer on the surface of the Fe_2O_3 spindles. After the Fe_2O_3 cores had been dissolved in HCl aqueous solution, uniform spindle hollow capsules were generated. The hollow carbon spindles can be fabricated through carbonization of the

PPy capsules. The formation mechanism and structural characteristics of the resulting core/shell and hollow spindles are discussed. Although we have only demonstrated this procedure with Fe_2O_3 core and polypyrrole shell as examples, we believe that this method should be extendible to other dimensions and to a range of other conductive shell materials. Since the hollow nature of the PPy and carbon capsules, they could have a wide range of applications, including catalysts, adsorbents, sensors, medicine carriers, and electrode materials.

2. Experimental

All chemicals are analytical grade and used as received without further purification.

2.1. Preparation and surface modification of spindle hematite cores

Monodispersed hematite spindles were obtained via aging the 2×10^{-2} M FeCl_3 and 4×10^{-4} M NaH_2PO_4 at 98°C for 3 days. The precipitate was centrifuged and washed several times with water and ethanol then dried under vacuum at 50°C . As-prepared spindle Fe_2O_3 nanoparticles were dispersed in ethanol by ultrasound. Then PVP (K_{30}) was dissolved into above solution and refluxing for 2 h. Un-adsorbed PVP was removed by several centrifugation/dispersion cycles at 3000 rpm.

2.2. Synthesis of spindle Fe_2O_3 @PPy core/shell particles and spindle PPy capsules

A typical synthesis of Fe_2O_3 @PPy ellipsoidal core/shell particles was carried out as follows: The modified spindle Fe_2O_3 nanoparticles (20 mg) were dispersed in deionized water (90 mL) via ultrasound. After these nanoparticles were well dispersed in the water, FeCl_3 (0.36 g)/ H_2O (10 mL) was added to the flask under vigorous stirring. 30 min later, pyrrole monomer (2.5×10^{-3} M) was injected into the solution. The polymerization was performed under stirring at 25°C for 8 h. After washing several times with distilled water and ethanol, the core/shell composites were dried under vacuum at 50°C . The Fe_2O_3 @PPy composite spindles were converted to PPy hollow capsules by soaking spindles in 1 M HCl aqueous solution.

2.3. Synthesis of carbon hollow capsules

The PPy hollow capsules were placed in a quartz tube, then vacuum sealed and heated at a heating rate of $1^\circ\text{C}/\text{min}$. After 3 h of carbonization at 900°C , the quartz tube was naturally cooled to room temperature. Carbon capsules were obtained after opening the sealed tube.

2.4. Characterization

X-ray powder diffraction patterns (XRD) of the products were obtained on a Japan Rigaku DMax- γ A rotation anode X-ray diffractometer equipped with graphite monochromatized

CuK α radiation ($\lambda = 1.54178 \text{ \AA}$). Transmission electron microscopy (TEM) photographs were taken on a Hitachi model H-800 transmission electron microscope at an accelerating voltage of 200 kV. The field emission scanning electron microscopy (FE-SEM) images were taken on a JEOL JSM-6700F SEM. X-ray photoelectron spectra XPS were measured on a photoelectron spectrometer using MgK α radiation. Infrared (IR) spectra were recorded in the wavenumbers range of 4000–500 cm^{-1} with a Nicolet Model 759 Fourier transform infrared (FT-IR) spectrometer using a KBr wafer. Raman spectrum of sample was taken at room temperature on a SPEX 1403 spectrometer. X-ray photoelectron spectra XPS were measured on a photoelectron spectrometer using MgK α radiation. Conductivity measurements were made on compressed pellets of dried powders using the conventional four-point probe technique at room temperature.

3. Results and discussion

3.1. Synthesis and surface modification of spindle Fe_2O_3 particles

The overall procedure for producing Fe_2O_3 /PPy ellipsoidal core/shell nanostructure and spindle hollow PPy nanostructure

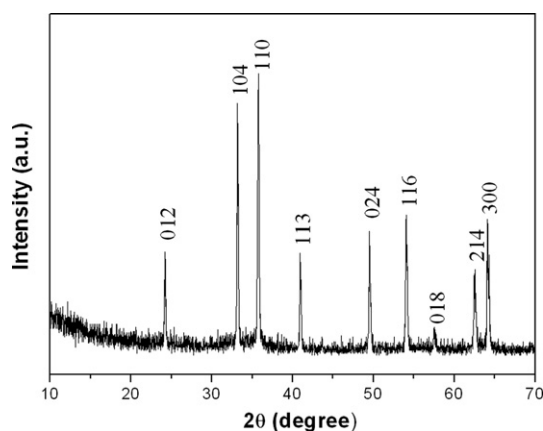


Fig. 1. XRD patterns of spindle $\alpha\text{-Fe}_2\text{O}_3$ particles.

involved several steps. The first step was the formation of spindle particles. Fe_2O_3 was chosen as the template not only for its non-spherical morphology, but also for it can be changed to magnetic Fe_3O_4 (our further work is to fabricate magnetic spindle capsules with magnetite core). Hematite nanoparticles with spindle morphology could be easily obtained via hydrolysis of FeCl_3 under controlling concentration, temperature and kind of ions used during the preparation process according to the Ohmori technique [27]. XRD pattern of the product is shown in Fig. 1, matching $\alpha\text{-Fe}_2\text{O}_3$ well from standard JCPDS date (86-0550). Fig. 2a displays a typical TEM micrograph for the spindle hematite particles. Its corresponding electron diffraction pattern (the inset of Fig. 2a) indicates the single-crystal nature of the sample. Fig. 2b is the SEM image of the same sample. The average size of the hematite particles is about 100–450 nm.

It is necessary to introduce proper kind of modifier to modify the spindle Fe_2O_3 nanoparticle for the fabrication of the core/shell nanostructure. Here, PVP macromolecule was invited as the modifier for its amphiphilic character which enables it dissolved in water or many other solvents [28]. Being an amphiphilic and non-ionic surfactant or steric stabilizer during many coating processes, hydrogen bond-like interactions are also possibly present between the hydrophilic part in PVP and the $-\text{OH}$ group of inorganic particles. It can have sufficient affinity of the core surface to the shell precursor so as to restrain secondary nucleation of shell material particles formed [26]. Being dispersed in PVP/ethanol solution via ultrasound, the Fe_2O_3 nanoparticles were effectively encompassed by PVP molecules, and the surface of the Fe_2O_3 nanoparticles may be sufficiently adsorbed by pyrrolidone ring of PVP. During the modification process, the refluxing played a key role to improve the adsorption of PVP onto the hematite particles by shielding the large Van der Waals forces between them. Although most of PVP macromolecules would be removed by later washing step, XPS measurement (Fig. 3a) shows that large amount of PVP molecules could be stably attached on the surface of the Fe_2O_3 nanoparticles for the atomic percent of the Fe atom was just 10%. This provides direct evidence for the strong absorption of PVP molecules on the surface of the spindle Fe_2O_3 nanopar-

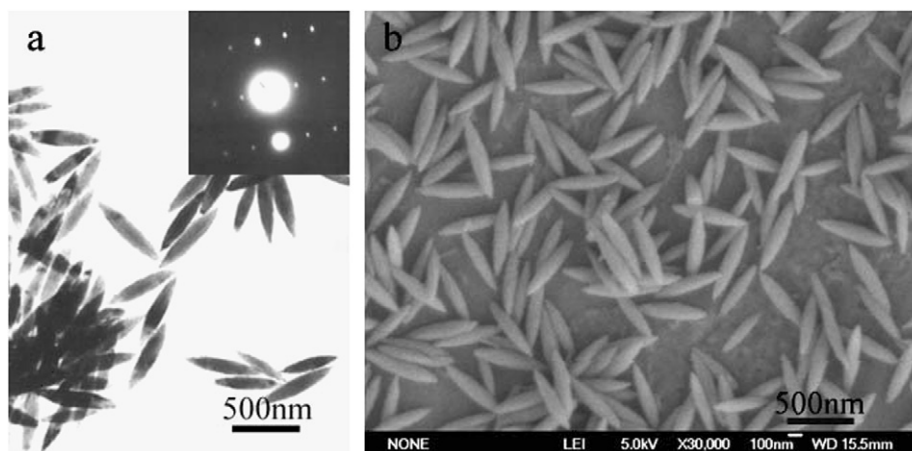


Fig. 2. TEM and SEM of the spindle $\alpha\text{-Fe}_2\text{O}_3$ particles.

ticles. Table 1 summarizes the atomic percent determined for PVP modified Fe_2O_3 particles. By comparison to PVP macromolecular, the N/C atomic ration is even lower, disagreement with the nitrogen content in the PVP repeat unit (theoretical ratio = 1:6). The reason may be response for that the $\text{C}_2\text{H}_5\text{OH}$ in our system were adsorbed on the surface of the Fe_2O_3 particles. The $\text{C}_2\text{H}_5\text{OH}$ anchored on the Fe_2O_3 surface, cause the enhancement of the carbon component. Compare to the adsorption modified method (keep other experiment parameters constant, just without refluxing), there are more PVP molecules attached on the surface of Fe_2O_3 particle by the XPS measurement (Table 1 and Fig. 3b). Obviously, the refluxing step is very important in our experiment, however, the real reason is not clear and more in-depth work should be done. Although the modified PVP layer promotes a strong interaction between the hydrophilic Fe_2O_3 surface and the hydrophobic PPy shell, them could not be observed by the TEM (Fig. 4c), despite they were effectively adsorbed on the surface of the Fe_2O_3 particles.

3.2. Fe_2O_3 @PPy core/shell spindles and hollow PPy capsules

In the process for the formation of Fe_2O_3 @PPy core/shell structure, FeCl_3 was invited as the initiator to oxidize pyrrole monomer. It was necessary to introduce FeCl_3 in the polymeric system before further add the pyrrole monomer, for the Fe^{3+} and PVP could form unstable complexes [29] which can further enhance the affinity between the Fe_2O_3 core and the nucleation of the PPy. After the in situ polymerization, PPy was successfully deposited on the spindle Fe_2O_3 nanoparticles to form core/shell structure. The typical TEM image (Fig. 4a) shows the core/shell nature of the product resulting from the above procedures. Well-defined particles were readily observed with light contrast PPy shells and dark contrast cores of Fe_2O_3 . No obvious changes in size or shape of Fe_2O_3 cores were observed and the Fe_2O_3 @PPy core/shell structure with well spindle mor-

phology was achieved. Fig. 4b depicts the typical SEM image of Fe_2O_3 @PPy spindles, shows that the core/shell products were well dispersed and the spindle morphology is well obtained, similar to the TEM results. The higher resolution SEM studies indicated that the PPy coating was relatively rough; see the inset of Fig. 4b. It is reported that smooth, uniform coatings were obtained on hydrophobic latexes whereas much more inhomogeneous coatings were observed on relatively hydrophilic latex particles [30–32]. In the present study, the non-uniform, granular nature of the PPy layer is readily distinguished from the smooth surface morphology of the Fe_2O_3 spindles (see Fig. 2b). Visual inspection of the PPy coated Fe_2O_3 particles confirmed some degree of flocculation compared to the original uncoated particles. This incipient flocculation may be caused by the PPy layer interfering with steric stabilization mechanism conferred by the PVP stabilizer.

To achieve a homogeneous layer of conductive PPy, various concentrations and deposition times were tested. It was found that higher concentrations of the reactants and longer deposition times resulted in a large amount of PPy aggregates on the surface of the spindle Fe_2O_3 cores. To reduce the formation of PPy aggregates, a very dilute solution with a monomer concentration were used in our experiment. In our system, when the amount of hematite spindle cores was fixed, the average thickness of the PPy shell was tunable from 15 to 35 nm by changing the pyrrole monomer concentration from 1.25×10^{-3} M to 2.5×10^{-3} M. Figs. 4b and 4c show two samples with different thicknesses of PPy shell. The surface roughness of the PPy layer and PPy aggregates attached to the Fe_2O_3 cores became more pronounced when the deposition time increased. Here, in our experiment, the optimum reaction time was 8 h. However, the pressed pellet conductivity of the Fe_2O_3 @PPy particles (35 nm shell thickness) was measured to be 2.1 S/cm, which is relatively low compared to the conductivities reported for Fe_2O_3 /PPy composites [33].

Spindle PPy capsules can be prepared from Fe_2O_3 @PPy core/shell particles by selective removal of Fe_2O_3 cores. Hollow PPy spindles were obtained after soaking the core/shell composites in hydrochloric acid. This means that the PPy shell was permeable to dissolution of the hematite core by HCl aqueous solution. The PPy capsules were characterized by TEM. The TEM image in Fig. 5 clearly shows the hollow spindle

Table 1
Apparent surface chemical composition as determined by XPS

Samples	C	N	O	Fe
Refluxing (a)	50.84	5.77	32.97	10.41
Adsorption (b)	40.80	3.00	36.90	19.40

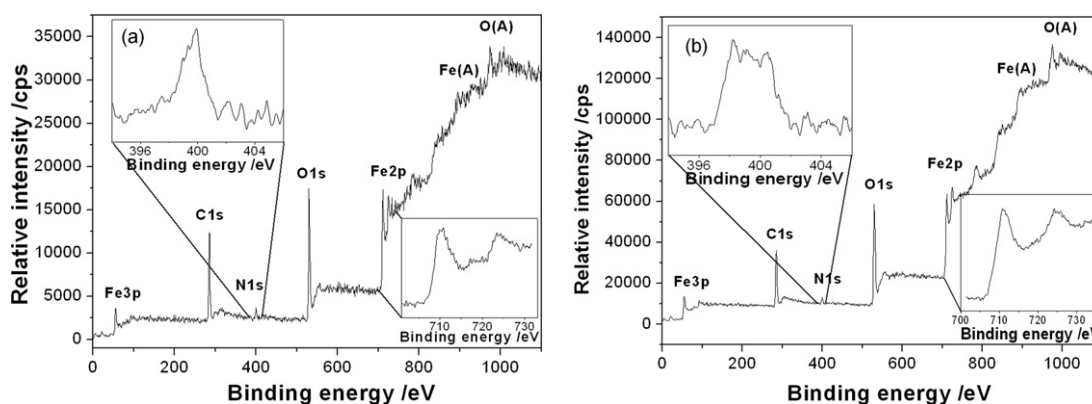


Fig. 3. XPS spectrum of PVP-modified spindle Fe_2O_3 particles by (a) refluxing, (b) adsorption.

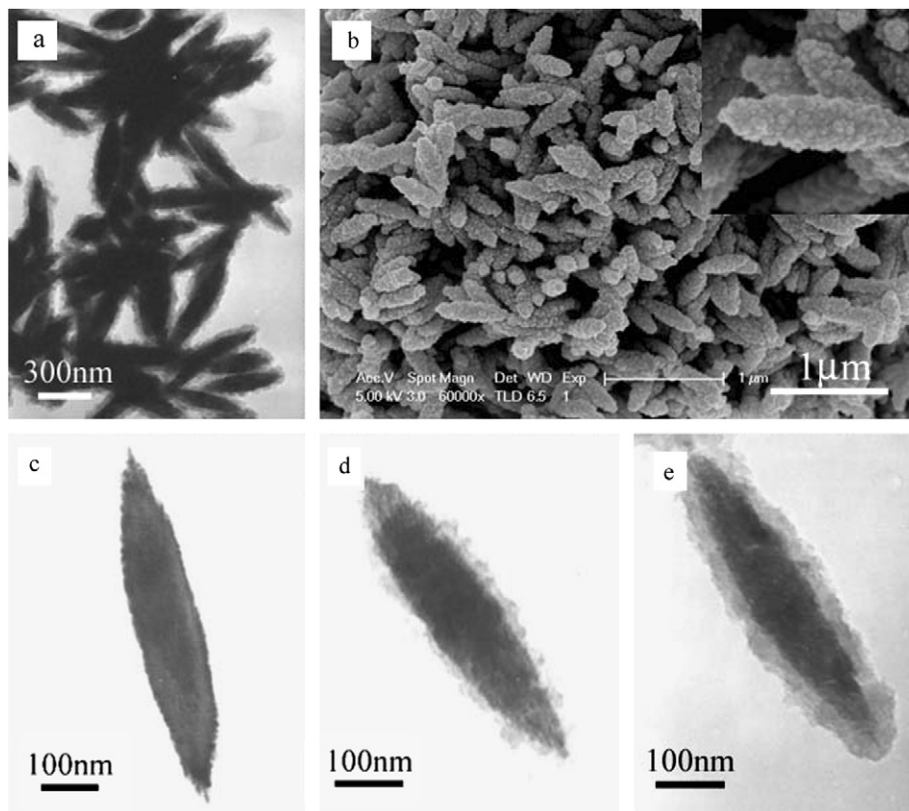


Fig. 4. Typical TEM (a) and SEM (b) images of the Fe_2O_3 @PPy spindles; and the product prepared at a concentration of (c) 0; (d) 1.25×10^{-3} and (e) 2.5×10^{-3} M of pyrrole in water.

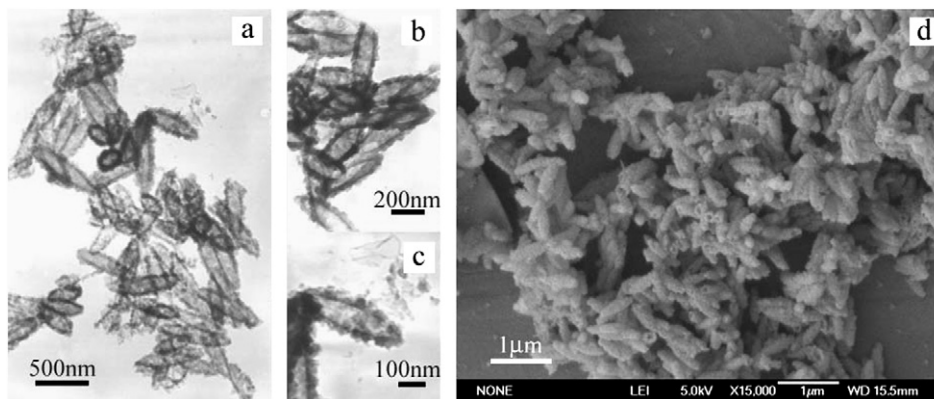


Fig. 5. Typical TEM (a, b, c) and SEM (d) images of the spindle PPy capsules.

structure of PPy in the majority of the material. SEM (Fig. 5d) was further invited to confirm the hollow nature of the capsules. The broken capsules in Fig. 5d reveal the hollow interior inside the PPy shell. In view of the well kept of the spindle morphology and thickness of the polymer shell, it is reasonable to confirm that the PPy shells are compact. The formation of PPy capsules after removal of the Fe_2O_3 cores also provides irrefutable evidence of the coaxial morphology of the Fe_2O_3 @PPy spindles.

FTIR spectroscopy proved to be useful to characterize the presence of the PPy coating on the surface of the Fe_2O_3 particles. The PVP modified Fe_2O_3 particles, Fe_2O_3 @PPy core/shell particles, PPy capsules and PPy powder (doped) were

analyzed by FT-IR as shown in Fig. 6. All the spectra were obtained from mixtures of samples with KBr in pellet form. In the spectrum of PPy powder (Fig. 6d), several characteristic broad bands were observed, particularly those at 1547 cm^{-1} and 1316 , 1186 , and 910 cm^{-1} in the 1000 – 1150 cm^{-1} region. These characteristic bands due to the PPy component were observed in the IR spectrum of Fe_2O_3 /PPy spindle particles (Fig. 6b), as expected. Additionally, a strong band at 570 cm^{-1} appears in the spectrum of Fe_2O_3 @PPy composites that is related to the Fe–O stretches in Fe_2O_3 . Analysis of the black PPy residue (Fig. 6c) after HCl treatment using FT-IR spectroscopy confirmed that this material was essentially PPy. No peak response to Fe_2O_3 was investigated in the PPy residue af-

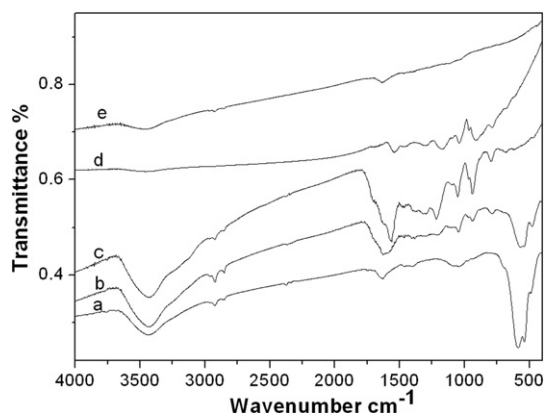


Fig. 6. FTIR spectra of (a) PVP-modified Fe_2O_3 , (b) Fe_2O_3 @PPy core/shell particles, (c) PPy capsules, (d) PPy powder, and (e) carbon capsules.

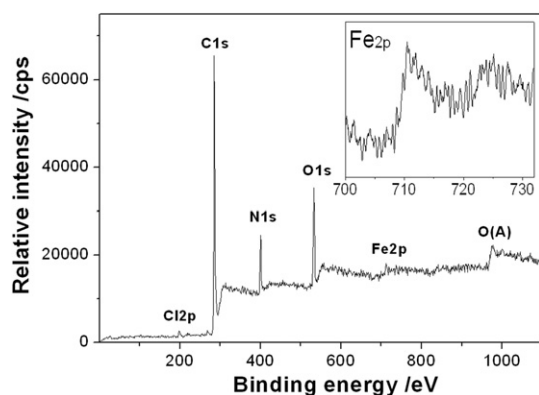


Fig. 7. XPS spectrum of the Fe_2O_3 @PPy core/shell spindles.

ter the HCl dissolution of Fe_2O_3 core. These results suggest that the PPy is effectively coated on the Fe_2O_3 particles.

In order to further verify the core/shell morphology of the PPy-coated Fe_2O_3 spindles, XPS was invited to gain evidence for the well core/shell nature. Fig. 7 shows the XPS spectra of the core/shell products. The main peaks are C1s, N1s, and O1s centered at 285, 400, and 532 eV, respectively. Particularly, one can note the increase in the N1s/O1s peak intensity ratio as the modified Fe_2O_3 spindles are coated with the PPy conducting polymer. This can easily be explained by the presence of high content of nitrogen in the PPy while the modified Fe_2O_3 particles only contain a small contribution of nitrogen brought by the PVP modifier. Similar to the previous report, new minor peaks appear in the core/shell spectrum, Cl2p (at 198 eV), is assigned to the chloride dopant. Further more, compare to the PVP modified Fe_2O_3 particles, the atomic ratio of the $\text{Fe}2p_{3/2}$ is remarkably decreased (about 0.62%, which may be assigned to the distribution of the iron in the form of FeCl_2 resulting from the reduction of the oxidizing agent Fe^{3+}). Thus, these XPS observation support that the Fe_2O_3 spindles are well coated by the PPy shell, which is further in agreement with the TEM and SEM analysis.

To understand the thermolysis process of Fe_2O_3 @PPy core/shell spindles, the thermal property of the core/shell products were investigated by TG under air (Fig. 8). The as-prepared sample showed a three-step weight loss in the temperature re-

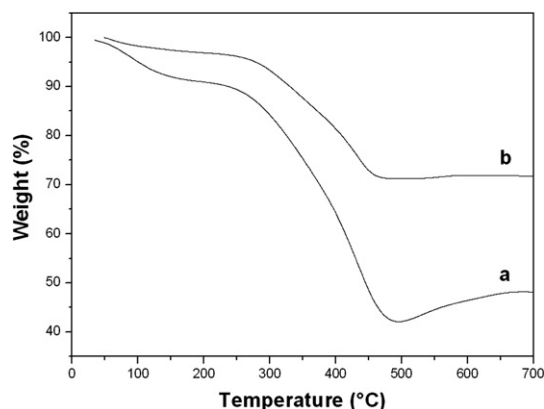


Fig. 8. TG of the Fe_2O_3 @PPy core/shell spindles with different shell thickness: (a) 15, (b) 35 nm.

gion of 40–700 °C. The initial weight loss from the core/shell composites up to 250 °C was probably due to removal of surface hydroxyls and/or surface adsorbed water, while the weight loss at higher temperature (250–500 °C) could be mainly attributed to the evaporation and subsequent decomposition of the PPy coating. It is very interesting to find that the weight is increasing while the temperature is higher than 500 °C. The reason can be explained as follows. It is reported that there are much gaseous byproducts such as CH_4 and HCN during the decomposition of the PPy [34], which may provide a reduced atmosphere. Many of these reduced gaseous products, which sealed in the spindle capsules by the compact PPy coating, may be reduced the hematite (Fe_2O_3) cores to give magnetic products such as Fe_3O_4 or Fe. As soon as the coating shell is burning out, the Fe_3O_4 or Fe will transfer to Fe_2O_3 and the weight will increase. Therefore, the obvious weight increase could be observed when the temperature is higher than 500 °C. From the TG analysis, the mass ratio of the Fe_2O_3 in the core shell composite with different shell thickness are about 48.2 and 71.7%, respectively.

3.3. Conversion to the spindle carbon capsules

Since PPy is one of the carbon sources [35], PPy hollow spindles can be converted to the corresponding carbon spindle capsules by thermal carbonization of the PPy shell. Fig. 9 shows the TEM and SEM images of the resulting carbon hollow spindles after thermal treatment of PPy capsules at 900 °C under a vacuum sealed tube. The SEM image (Fig. 9c) shows that the carbon capsules not only possess unique spindle morphology but are also very uniform in size. Moreover, the broken capsules also revealed the hollow structure of these particles. The TEM micrograph in Fig. 9a further evidences the hollow nature of the carbon spindles with a sharp contrast between the dark edge and the pale center. The spindle shell thickness, determined from the TEM image (Fig. 9b), is approximately 27 nm. The carbon nanocapsules showed a reduced shell thickness (ca. 8 nm). The shrinkage in the sizes results from the formation of more compact structures accompanied by denitrogenation, dehydrogenation and aromatization in the carbonization process [36,37].

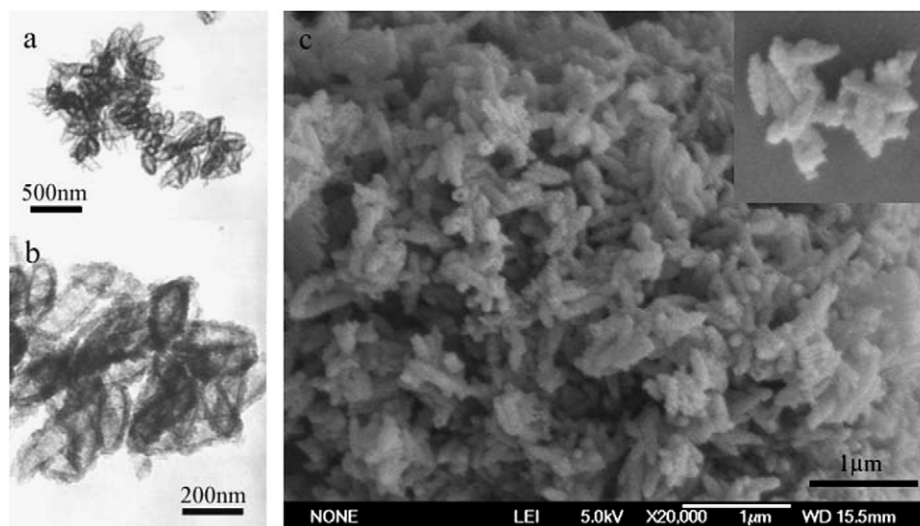


Fig. 9. Typical TEM (a, b) and SEM (c) images of the spindle carbon capsules.

The electron diffraction pattern exhibits fuzzy rings (not show), indicating that the carbon produced from pyrolyzing PPy at 900 °C has a low crystallinity. It has been reported that when carbonized at 2400 °C, a highly crystalline carbon material with high conductivity occurs through the carbonization process [38]. A typical Raman spectrum is shown in Fig. 10, where a prominent peak at 1591 cm^{-1} and another relatively weak peak at 1351 cm^{-1} can be clearly found. The peak at 1591 cm^{-1} (G-band) is attributed to the stretching modes of carbon sp^2 bonds of the typical graphite (E_{2g} mode), while the peak at 1351 cm^{-1} (D-band) is associated with the vibrations of carbon atoms with dangling bonds in disordered graphite planes [39]. The relative intensity (I_D/I_G) of carbon capsules carbonized at 900 °C was 1.0. This intensity ratio indicates a semicrystalline carbon structure containing some lattice edges or plane defects within the analyzed carbon nanocapsules [39,40]. To further confirm the conversion to the carbon materials, the FTIR spectrum was studied. All the peaks in the IR spectra (Fig. 6e) of PPy capsules were removed completely following the thermal treatment. A featureless IR spectrum resulted as expected for the carbon capsules. This suggests that all the functional groups in PPy have been eliminated, leaving behind symmetric carbon that shows no IR absorption in this region.

4. Conclusion

In summary, spindle Fe_2O_3 @PPy core/shell particles, PPy capsules and carbon capsules have been successfully prepared using the surface-modified templating method. The preparation of Fe_2O_3 @PPy core/shell spindles involves the fabrication of Fe_2O_3 spindles as core templates, surface modification and in situ deposition of PPy on the Fe_2O_3 spindles. The average thickness of the PPy shell was tunable from 15 to 35 nm by changing the pyrrole monomer concentration from 1.25×10^{-3} to 2.5×10^{-3} M. And the optimum reaction time in our system was 8 h. Both the TEM and SEM studies revealed the spindle morphology for the PPy residues following acid treatment.

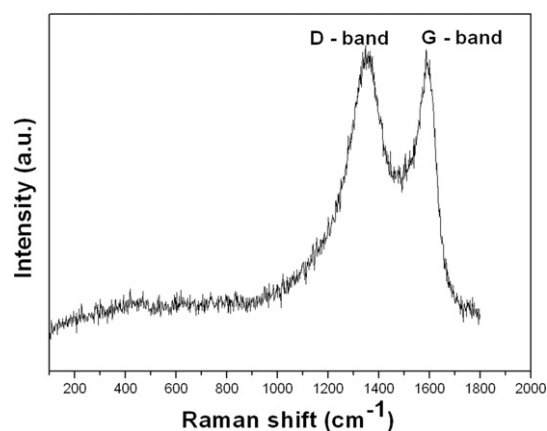


Fig. 10. Raman spectrum of the spindle carbon capsules.

Furthermore, the PPy hollow capsules can be converted into carbon hollow spindles by thermolysis at 900 °C. It is the first report of the Fe_2O_3 @PPy core/shell particles, PPy capsules and carbon capsules with spindle morphology. And these new materials open up opportunities for the development of new carriers for drugs and catalysts.

Acknowledgments

We gratefully acknowledge financial support from the Specialized Research Fund for the Doctoral Program of Higher Education (SRFDP, 20040358056) and the Postdoctoral Fund (No. 20060390689) of China.

References

- [1] F. Caruso, Adv. Mater. 13 (2001) 11.
- [2] I. Gill, A. Ballesteros, J. Am. Chem. Soc. 120 (1998) 8587.
- [3] Z.Y. Zhong, Y.D. Yin, B. Gates, Y. Xia, Adv. Mater. 12 (2000) 206.
- [4] M.S. Fleming, T.K. Mandal, D.R. Walt, Chem. Mater. 13 (2001) 2210.
- [5] T. Hirakawa, P.V. Kamat, Langmuir 20 (2004) 5645.
- [6] L.M. Liz-Marzan, M. Giersig, P. Mulvaney, Langmuir 12 (1996) 4329.
- [7] F. Caruso, R.A. Caruso, H. Möhwald, Science 282 (1998) 1111.

- [8] S.M. Marinakos, J.P. Novak, L.C. Brosseau, A.B. House, E.M. Edeki, J.C. Feldhaus, D.L. Feldheim, *J. Am. Chem. Soc.* 121 (1999) 8518.
- [9] H. Dou, M. Jiang, H. Peng, D. Chen, Y. Hong, *Angew. Chem. Int. Ed.* 42 (2003) 1516.
- [10] Y. Hu, X. Jiang, Y. Ding, Q. Chen, C. Yang, *Adv. Mater.* 16 (2004) 933.
- [11] P. Jiang, J.F. Berton, V.L. Colvin, *Science* 291 (2001) 453.
- [12] S.W. Kim, M. Kim, W.Y. Lee, T. Hyeon, *J. Am. Chem. Soc.* 124 (2002) 7642.
- [13] D.B. Cairns, S.P. Armes, L.G.B. Bremer, *Langmuir* 15 (1999) 8052.
- [14] C. Barthet, S.P. Armes, M.M. Chehimi, C. Bilem, M. Omastova, *Langmuir* 14 (1998) 5032.
- [15] S. Fujii, S.P. Armes, R. Jeans, R. Devonshire, S. Warren, S.L. McArthur, M.J. Burchell, F. Postberg, R. Srama, *Chem. Mater.* 18 (2006) 2758.
- [16] L. Cen, K.G. Neoh, Y.L. Li, E.T. Kang, *Biomacromolecules* 5 (2004) 2238.
- [17] S.F. Lascelles, S.P. Armes, *Adv. Mater.* 7 (1995) 864.
- [18] M.L. Abel, M.M. Chehimi, A.M. Brown, S.R. Leadley, J.F. Watts, *J. Mater. Chem.* 5 (1995) 845.
- [19] L.Y. Hao, C.L. Zhu, C.N. Chen, P. Kang, Y. Hu, W.C. Fan, Z.Y. Chen, *Synth. Met.* 139 (2003) 391.
- [20] X.M. Yang, T.Y. Dai, Y. Lu, *Polymer* 47 (2006) 441.
- [21] D.M. Cheng, H.B. Xia, H.S.O. Chan, *Nanotechnology* 17 (2006) 1661.
- [22] L. Gabrielson, M.J. Folkes, *J. Mater. Sci.* 36 (2001) 1.
- [23] T.D. Burchell, *Carbon Materials for Advanced Technologies*, Pergamon, Oxford, UK, 1999.
- [24] J. Jang, X.L. Li, J.H. Oh, *Chem. Commun.* 7 (2004) 794.
- [25] X.M. Sun, Y.D. Li, *Langmuir* 21 (2005) 6019.
- [26] L.Y. Hao, C.L. Zhu, W.Q. Jiang, C.N. Chen, Y. Hu, Z.Y. Chen, *J. Mater. Chem.* 14 (2004) 2929.
- [27] M. Ohmori, E. Maijevic, *J. Colloid Interface Sci.* 160 (1993) 288.
- [28] C. Graf, D.L.J. Vossen, A. Imhof, A. Blaaderen, *Langmuir* 19 (2003) 6693.
- [29] M. Liu, X. Yan, H. Liu, W. Yu, *React. Funct. Polym.* 44 (2000) 55.
- [30] S.F. Lascelles, S.P. Armes, *J. Mater. Chem.* 7 (1997) 1339.
- [31] S.F. Lascelles, S.P. Armes, P. Zhdan, S.J. Greaves, A.M. Brown, J.F. Watts, S.R. Leadley, S.Y. Luk, *J. Mater. Chem.* 7 (1997) 1349.
- [32] D.B. Cairns, M.A. Khan, C. Perruchot, A. Riede, S.P. Armes, *Chem. Mater.* 15 (2003) 233.
- [33] R. Gangopadhyay, A. De, *Eur. Polym. J.* 35 (1999) 1985.
- [34] C.C. Han, J.T. Lee, R.W. Yang, C.H. Han, *Chem. Mater.* 13 (2001) 2656.
- [35] C.C. Han, J.T. Lee, R.W. Yang, C.H. Han, *Chem. Mater.* 11 (1999) 1806.
- [36] J. Jang, J.H. Oh, *Chem. Commun.* 7 (2004) 882.
- [37] E. Ando, S. Onodera, M. Iino, O. Ito, *Carbon* 39 (2001) 101.
- [38] C. Han, J. Lee, H. Chang, *Chem. Mater.* 13 (2001) 4180.
- [39] M.S. Dresselhaus, G. Dresselhaus, M.A. Pimenta, P.C. Eklund, in: M.J. Pelletier (Ed.), *Analytical Applications of Raman Spectroscopy*, Blackwell, Oxford, UK, 1999, chap. 9.
- [40] J. Jang, J.H. Oh, X.L. Li, *J. Mater. Chem.* 14 (2004) 2872.